Topological Chaos and Periodic Braiding of Almost-Cyclic Sets

Mark A. Stremler, Shane D. Ross, Piyush Grover, and Pankaj Kumar

Topological chaos and periodic braiding of almost-cyclic sets

Mark A. Stremler, Shane D. Ross, Piyush Grover, Pankaj Kumar

Engineering Science and Mechanics, Virginia Tech, Blacksburg, Virginia, 24061, USA

In certain (2+1)-dimensional dynamical systems, the braiding of periodic orbits provides a framework for analyzing chaos in the system through application of the Thurston-Nielsen classification theorem. Periodic orbits generated by the dynamics can behave as physical obstructions that 'stir' the surrounding domain and serve as the basis for this topological analysis. We provide evidence that, even in the absence of periodic orbits, almost-cyclic regions identified using a transfer operator approach can reveal underlying structure that enables topological analysis of chaos in the domain.

There is much interest in understanding how chaos arises in dynamical systems, how to detect it, and how to design for (or against) it [1]. This perspective has proven important in many areas of the physical sciences, including atomic physics [2], climate modeling [3], and astronomy [4]. In fluid mechanics, the presence of chaotic fluid particle trajectories is often associated with enhanced mixing [5]. Chaotic trajectories can be produced by deterministic, regular velocity fields, making this approach a particularly important tool for analyzing very viscous and/or small-scale fluid transport [6], but the principles apply to flows at any scale.

One recent approach to analyzing chaos in a fluid system is the identification of 'topological chaos', or chaos due to topology of internal boundary motions such as moving rods [7, 8]. This approach is based on application of the Thurston-Nielsen classification theorem [9] (TNCT) to certain (2+1)-dimensional flows: either two-dimensional, time-dependent flows or three-dimensional flows that, because of symmetry, can be cast as surface homeomorphisms (i.e. two-dimensional mappings) [10]. The TNCT provides quantitative lower bounds on maximum stretching rates in such flows using only information from the boundary motions. 'Ghost rods', or periodic orbits generated by the dynamics, can also behave as physical obstructions that 'stir' the surrounding fluid, providing a basis for the topological analysis in place of physical boundaries [11]. A similar classification of strange attractors is given by the relative rotations rates and linking numbers for embedded periodic orbits [12]. With these topological approaches it is possible to observe the motion of a small number of objects, be they physical obstructions or ghost rods, and from the topology of their trajectories infer what possible, but otherwise unobserved, motions are present in the system.

The analysis of dynamical systems using the TNCT has been largely dependent on the presence and identification of exactly periodic orbits [11, 13]. Recently the analysis of ghost rod topology in a fluid has been extended to aperiodic orbits [14, 15], relaxing a substantial restriction in the application of the TNCT. However, this approach introduces the complexity of needing to iden-

tify appropriate aperiodic orbits, as a random selection of trajectories generally leads to a poor estimate of the overall system behavior [14].

Here we apply the TNCT based on the presence of almost-cyclic sets. Almost-cyclic sets (ACS) [16] are closely related to almost-invariant sets (AIS) [17], which define macroscopic structures preserved by the dynamics. This generalization is an important step in making the analysis of topological chaos using the TNCT applicable to a wider range of problems, including more complex fluid systems [18] and other dynamical systems that can be represented as surface homeomorphisms [2, 4].

We first give a description of the example system we use to examine the role of ACS in topological chaos, and we demonstrate application of the TNCT to a reference case in which there exist low-order periodic orbits. We then show that an eigenfunction of the Perron-Frobenius operator associated with this system is an ACS with topological properties that give an estimate of the measured topological entropy, even when the system is perturbed so that appropriate periodic particle trajectories no longer exist. That is, periodic motion of ACS, instead of directly observed particle trajectories, can identify ghost rods for application of the TNCT.

For simplicity of exposition, we examine a flow having an exact mathematical representation. Consider time-dependent Stokes flow [19] in the domain $M = \{(x,y) : 0 \le x \le 2a, -b \le y \le b\}$ shown in Fig. 1. Flow is driven by a tangential velocity along the bottom boundary

$$V(x,t) = U_1 \sin\left(\pi x/2\,a + \phi\right) + U_2 \sin\left(\pi x/a + 2\,\phi\right),$$

$$\phi(t) = \begin{cases} \pi & \text{for } t \in [n\tau_f, (n+1)\tau_f/2), \\ 0 & \text{for } t \in [(n+1)\tau_f/2, (n+1)\tau_f), \end{cases}$$

where n is an integer, and a tangential velocity along the top boundary given by $-V(x,t)$, so that the flow pattern is symmetric about $y = 0$. The (otherwise steady) flow pattern is reflected about $x = a$ every $t = n\tau_f/2$. The mathematical representation for this flow is a closed-form solution of the biharmonic equation for the streamfunction $\psi(x,y,t)$ [20]. This system is a variation on the classic double-lid-driven cavity flow [21], with the side boundaries taken to be free surfaces [22] and with the top and
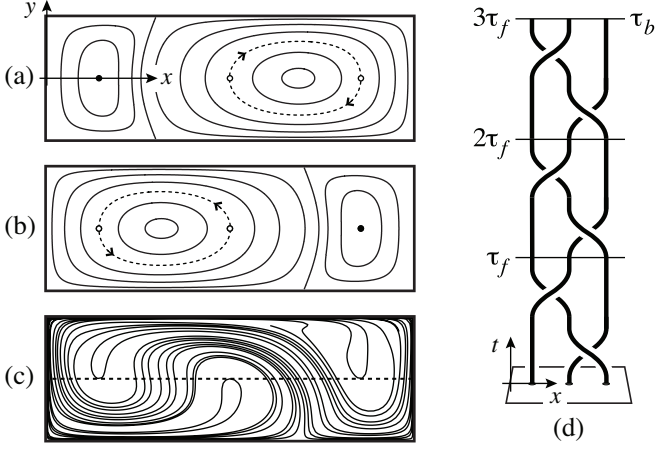
FIG. 1. Streamlines in the model flow for (a) $t \in [n\tau_f, (n+1)\tau_f/2]$ and (b) $t \in [(n+1)\tau_f/2, (n+1)\tau_f]$. Solid circles mark fixed points at $(a \mp x_s, 0)$; open circles mark points at $(a, 0)$ and $(a \pm x_s, 0)$ that move along the dotted streamlines. (c) Stretching of a material line initially along the x-axis (dashed line) after three periods of the flow (solid line). (d) The mathematical braid on 3 strands representing the period-3 orbits as viewed from $y < -b$.

bottom boundaries each having two regions of opposing motion. A similar model has been used to study counter-rotating flow in a channel due to herringbone-patterned surface grooves [23].

The motion of a passive (i.e. non-diffusive, inertialess, drag-free) particle in this system is given by solution of $d\mathbf{x}/dt = \mathbf{V}(\mathbf{x}, t)$, where $\mathbf{x}(t) = (x, y)$ is the particle position and $\mathbf{V}$ is the velocity field defined by $\mathbf{V} = (\partial\psi/\partial y, -\partial\psi/\partial x)$. While the fluid system is viscous, and thus is dissipative, passive particle motions in this time-periodic, area-preserving flow comprise a conservative Hamiltonian system.

Throughout this Letter we focus on the aspect ratio $a/b = 3$ and the velocity ratio $U_2/U_1 \approx 0.841$, which gives counter-rotating streamline patterns as shown in Fig. 1. The value of U_2/U_1 is chosen so that the points $(a, 0)$ and $(a + x_s, 0)$ in Fig. 1(a) lie on the same streamline and $(a - x_s, 0)$ is a fixed point. Perturbations in a/b and U_2/U_1 can be considered, but we do not do so here. We begin our discussion with $a = \pi$, $U_1 \approx 9.928$, and $\tau_f = \tau_f^* = 1.0$, which we refer to as our 'reference case'. With this special choice of parameters, passive particles located initially at $(a, 0)$ and $(a + x_s, 0)$ have exactly exchanged position when $t = \tau_f^*/2$. The flow pattern is then reflected about $x = a$, as shown in Fig. 1(b), and the fluid particles located at $(a - x_s, 0)$ and $(a, 0)$ when $t = \tau_f^*/2$ have exactly exchanged position when $t = \tau_f^*$. This sequence of flow patterns is then repeated, and these three points along the x-axis lie on period-3 orbits of the flow. The response of this system to perturbations in the value of τ_f is a central theme of this discussion.

Braid theory provides a framework for discussing the topology of periodic orbits, with the space-time trajec-

tory of each orbit represented by a single braid strand. In our reference case, the period-3 orbit trajectories can be represented by the braid shown in Fig. 1(d). Since it is the topology of the braid that is classified by the TNCT, it is the direction and sequence of the strand interchanges, not the actual dynamics along the trajectories, that are essential in the analysis. Each strand returns to its initial position every $\Delta t = 3\tau_f = \tau_b$, which gives one period of the braid. The topology of this braid is identical to that in [7, 13].

According to the TNCT, the braid in Fig. 1(d) is of *pseudo-Anosov* (pA) type. That is, the underlying flow map is topologically equivalent (i.e., isotopic) to an ideal pA map that, except for a finite number of singularities, stretches everywhere in the unstable direction by a factor $\lambda_{\mathrm{TN}} > 1$ and contracts everywhere in the stable direction by a factor $1/\lambda_{\mathrm{TN}}$ [7, 10]. In the ideal case, material lines throughout the domain grow as λ_{TN}^p, where p is the (integer) period of the braid. This chaotic behavior is preserved under any continuous deformation of the domain that maintains the topology of the periodic orbit trajectories [24], so in our reference case a subdomain of the fluid is subjected to exponential stretching at a rate that is at least λ_{TN}. Thus, the TNCT provides a lower bound on the topological entropy of the flow, $h = \ln(\lambda)$, where $\lambda \geq \lambda_{\mathrm{TN}}$ is the maximum line-stretching exponent over all possible initial material lines. The size of the relevant subdomain is not predicted by the TNCT, but experimental results indicate that this region is typically on the scale of the orbit motions [7].

For the braid in Fig. 1(d), the TNCT gives $\lambda_{\mathrm{TN}} = (3 + \sqrt{5})/2$, or $h_{\mathrm{TN}} = \ln(\lambda_{\mathrm{TN}}) \approx 0.962$. The actual topological entropy of this flow can be determined by computing the asymptotic stretching rate of topologically nontrivial lines [25], such as lines that join a periodic point with the outer boundary. For the reference case we compute $h \approx 0.968$, which is well represented by h_{TN}. In general, if the braid representing periodic orbits in a flow is of pA type, this small amount of topological data establishes a quantitative lower bound on the complexity in the dynamics of the flow.

In [7], the fluid motion is generated by causing solid rods to move along a pA braid. Here, the periodic orbits of the braid are driven by the flow. Despite the passive nature of the braid in this case, the stretching and folding pattern in the surrounding fluid, Fig. 1(c), is similar to that generated by actual rods moving through the flow (cf. Fig. 2 in [7]). Periodic orbits such as these have thus been termed 'ghost rods' [11].

Varying the value of τ_f away from τ_f^* prevents the points identified in Fig. 1 from exactly exchanging position during one period of the flow, and these points no longer lie on period-3 orbits. Increasing τ_f causes each of the periodic points in the reference case to bifurcate into a set of two hyperbolic points and two elliptic points, as in Fig. 2(b). These four points travel together through
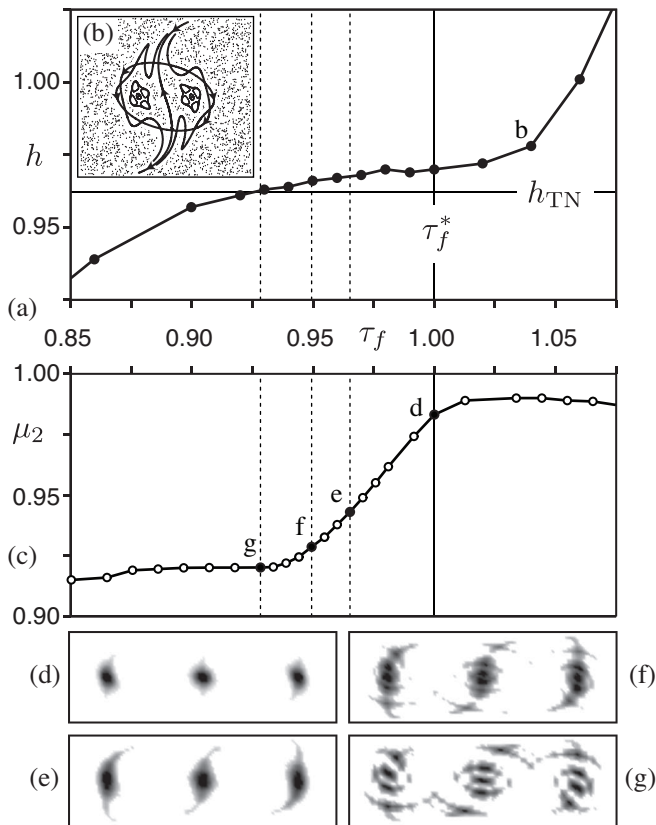
FIG. 2. (a) Topological entropy for the flow. Error bars are covered by each data point. Inset (b) shows portions of the stable and unstable manifolds of the hyperbolic periodic points the Poincaré section in the center of the domain for $\tau_f = 1.04$. (c) Variation in μ_2, the second-largest eigenvalue for τ_f^*. AIS determined by the corresponding eigenvector ν_2 are shown for τ_f (d) = 1, (e) ≈ 0.965, (f) ≈ 0.95, and (g) ≈ 0.93. The elements of ν_2 (with components ν_{2i}) are colored according to magnitude on a linear grayscale from white (for $\nu_{2i} \leq 0.01$) to black (for $\nu_{2i} \geq 0.85$).

creases, we adopt a set-oriented approach for identifying almost periodic behavior in the dynamics. In this approach, the domain (or phase space) is decomposed into subsets such that a typical trajectory has a very small probability of moving between subsets in a short time. In our example there are two subsets, or almost-invariant sets (AIS), one of which is a disconnected set of three components that map one to another; these components are the almost-cyclic sets (ACS) of interest. The other subset is its phase space complement. The space-time trajectories of the ACS are periodic, even though all particle trajectories are likely to 'leak' from these sets (for $\tau_f < \tau_f^*$) if given sufficient time.

We compute the AIS, and hence the ACS, using the discretized Perron-Frobenius transfer operator, P_{t,τ_f}, which we approximate using a multi-dimensional Ulam's method [16, 26]. From P_{t,τ_f} we form a reversible matrix R_{t,τ_f} and determine its eigenspectrum [27]. This eigenspectrum provides insight into the various AIS present in the system [17]. The first eigenvector, ν_1, corresponding to the eigenvalue $\mu_1 = 1$, is the invariant (uniform) distribution of the system. The AIS of interest are isolated by the (near) zero contour of the eigenvector ν_2, which corresponds to the second largest eigenvalue $\mu_2 < 1$. The magnitude of μ_2 gives a measure of the invariance, or 'leakiness' of this AIS [17]. In general, one can also consider the AIS given by lower ranked eigenvectors of R_{t,τ_f}, which capture increasingly smaller scale structures [28]. For this flow, the ν_2 eigenvector family captures the dominant braiding for the range of τ_f considered.

The eigenvector ν_2 for the reference case is shown in Fig. 2(d). The AIS in this case is a collection of three ACS that form around the three periodic points. The space-time trajectories of the ACS track the periodic orbits and thus can be represented by the same braid. Consider now the change in structure of ν_2 as the value of τ_f is decreased from τ_f^* [29]. Figure 2(c) shows that as τ_f decreases, μ_2 decreases, indicating that the ACS become more leaky. As illustrated in Fig. 2(e), for $0.965 \lesssim \tau_f < 1$, the flow still contains three ACS despite the fact that these sets do not contain any period-3 orbits, and the relative motion of the ACS 'shadows' that of the (now nonexistent) periodic orbits [30]. While the fluid in these sets eventually leaks out, by definition there are particles that move with the ACS for a significant length of time. The braid representing the relative motion of these particles is isotopic to the braid in Fig. 1(d) over the length of time these particles remain in the ACS. The infinite-time braid of these particles is almost certainly aperiodic, but the entropy of the finite-time braid, particularly when shared by a number of different particles, provides a good representation of the actual entropy of the flow [15]. Thus, the entropy predicted by the braid of the ACS, h_{TN}, gives an accurate lower bound on the actual entropy of the flow h, as shown in Fig. 2(a).

The three ACS identified for $0.965 \lesssim \tau_f \leq 1$ begin to

the flow, twisting around one another as they move, and one can view these four trajectories as forming a single twisted strand. The collective motion of these 12 periodic orbits is thus similar to that of the three periodic orbits in the reference case, and the perturbed flow can be represented by a braid that is *reducible* to the pA braid in Fig. 1(d). For large τ_f, the energy added to the flow leads to additional stretching and folding beyond that predicted by the TNCT, but Fig. 2(a) shows that $h_{TN} \approx 0.962$ remains a good estimate of the flow behavior for roughly a 5% increase in τ_f and remains a lower bound on h for all $\tau_f > \tau_f^*$ considered here.

In contrast, perturbing τ_f below τ_f^* removes the low-order periodic orbits that can readily be identified as ghost rods. However, it is clear from the data in Fig. 2(a) that h_{TN} from the reference case continues to provide a lower bound on h for roughly a 5% decrease in τ_f, despite the fact that there are no longer any period-3 orbits on which to base the topological analysis.

To explain this persistence of stretching as τ_f de-

break up around $\tau_f \approx 0.95$, Fig. 2(f), and when $\tau_f \approx 0.93$ the flow appears to contain 13 ACS, Fig. 2(g), that generate a new braid with a lower entropy. This breakup of the three ACS corresponds quite closely to the entropy of the flow, h, dropping below h_{TN}, the lower bound based on the presence of a braid isotopic to that in Fig. 1(d).

Periodic motion of 'ghost rods' can reveal and quantify the presence of exponential stretching and folding in the surrounding flow without requiring detailed information about the full flow field. The standard approach to identifying chaos relies on long-time observations of chaotic motion. This topological approach identifies chaos based on relatively short-time observations of *regular* motion. As we have demonstrated, these ghost rods need not be found by direct observation of invariant objects — periodic motion of ACS can reveal the topological structure needed for application of the TNCT. Thus, identification and quantification of chaos can be based on limited data regarding the regular motion of finite regions of the flow that move together for only a finite time [31].

While we have discussed the role of ACS as ghost rods in the context of fluid stirring, many dynamical systems can be cast as periodic homeomorphisms of a disk and thus viewed as a flow. AIS have been observed in numerous systems [28, 32, 33], even those exhibiting stochastic behavior [34]. Our results show that the relative motion of distinct components of an AIS, i.e. the ACS, can be viewed as a braid in space-time and analyzed using the Thurston–Nielsen classification theorem. This connection between set-oriented methods and the TNCT promises to provide a powerful tool for investigating transport in a variety of dynamical systems.

[1] M. C. Cross and P. C. Hohenberg, Rev. Mod. Phys. **65**, 851 (1993).
[2] C. Jaffé, D. Farrelly, and T. Uzer, Phys. Rev. A **60**, 3833 (1999).
[3] R. T. Pierrehumbert, Geophys. Astrophys. Fluid Dyn. **58**, 285 (1991).
[4] W. S. Koon et al. Chaos **10**, 427 (2000).
[5] H. Aref, Phys. Fluids **14**, 1315 (2002).
[6] M. A. Stremler, F. R. Haselton, and H. Aref, Phil. Trans. R. Soc. Lond. A **362**, 1019 (2004).
[7] P. L. Boyland, H. Aref, and M. A. Stremler, J. Fluid Mech. **403**, 227 (2000).
[8] J.-L. Thiffeault and M. D. Finn, Phil. Trans. R. Soc. A **364**, 3251 (2006).
[9] W. P. Thurston, Bull. Am. Math. Soc. **19**, 417 (1988).
[10] P. L. Boyland, Topology and Its Applications **58**, 223 (1994).
[11] E. Gouillart, J.-L. Thiffeault, and M. D. Finn, Phys. Rev. E **73**, 036311 (2006).
[12] G. B. Mindlin et al. Phys. Rev. Lett. **64**, 2350 (1990).
[13] M. A. Stremler and J. Chen, Phys. Fluids **19**, 103602 (2007); J. Chen and M. A. Stremler, Phys. Fluids **21**, 021701 (2009).
[14] J.-L. Thiffeault, Phys. Rev. Lett. **94**, 084502 (2005).
[15] J.-L. Thiffeault, Chaos **20**, 017516 (2010).
[16] M. Dellnitz and O. Junge, SIAM J. Num. Anal. **36**, 491 (1999).
[17] M. Dellnitz et al. Int. J. Bifurc. Chaos **15**, 699 (2005).
[18] P. Okely, J. Imberger and K. Shimizu, Limn. Ocean. **55**, 589 (2010).
[19] That is, flow for which the Reynolds number, Re $= VL/\nu$, is taken to be the limiting case Re $= 0$, where ν is the kinematic viscosity, V is a characteristic velocity, and L is a characteristic length.
[20] V. V. Meleshko and A. M. Gomilko, Proc. R. Soc. London A **460**, 807 (2004). [Our choice of boundary conditions allows for an exact solution with a finite number of terms.]
[21] W. L. Chien, H. Rising and J. M. Ottino, J. Fluid Mech. **170**, 355 (1986).
[22] P. Gaskell et al. J. Fluid Mech. **298**, 113 (1995).
[23] A. D. Stroock and G. J. McGraw, Phil. Trans. R. Soc. London A **362**, 971 (2004).
[24] M. Handel, Ergodic Theory and Dynamical Systems **5**, 373 (1985).
[25] S. Newhouse and T. Pignataro, J. Stat. Phys. **72**, 1331 (1993).
[26] J. Ding, T. Y. Li, and A. Zhou, J. Comp. Appl. Math **147**, 137 (2002).
[27] G. Froyland and K. Padberg, Physica D **238**, 1507 (2009).
[28] G. Froyland et al. Phys. Rev. Lett. **98**, 224503 (2007).
[29] O. Junge, J. E. Marsden, and I. Mezic, in *Proc. 43rd IEEE Conf. Decision Control*, p. 2225 (2004).
[30] M. Shub, *Global Stability of Dynamical Systems* (Springer-Verlag, 1987).
[31] The accuracy of the lower bound predicted by the TNCT depends on the underlying system and the braid being used in the analysis. The excellent correspondence here between h and h_{TN} is a feature of the simple flow we have used to illustrate this approach.
[32] P. Deuflhard et al. in *Molecular Dynamics: Challenges, Methods, Ideas*, Vol. 4, edited by P. Deuflhard et al. (Springer-Verlag, 1998), p. 98.
[33] M. Dellnitz et al. Phys. Rev. Lett. **94**, 231102 (2005).
[34] L. Billings and I. B. Schwartz, Chaos **18**, 023122 (2008).